Object size effect on the contact potential difference measured by scanning Kelvin probe method

B. Polyakov, R. Krutokhvostov, A. Kuzmin, E. Tamanis, I. Muzikante, I. Tale

Object size effect on the contact potential difference measured by scanning Kelvin probe method

B.Polyakov[1], R.Krutokhvostov[1], A.Kuzmin[1], E.Tamanis[2], I.Muzikante[1], I.Tale[1]

[1]Institute of Solid State Physics, University of Latvia,

Kengaraga st. 8, LV-1063, Riga, Latvia,

[2]G.Liberta Innovative Microscopy Center, Daugavpils University, Parades street 1,

LV-5401, Daugavpils, Latvia,

Fax: (+371) 7132778, Phone: (+371) 26718631, E-mail: boris.polyakov@cfi.lu.lv

Abstract

Contact potential difference (CPD) was measured by macroscopic Kelvin probe instrument and scanning Kelvin probe microscope on Al, Ni and Pt on ITO substrates at ambient conditions. CPD values measured by scanning Kelvin probe microscope and macroscopic Kelvin probe are close within the error of about 10-30% for large studied objects, whereas scanning Kelvin probe microscope signal decreases, when the object size becomes smaller than 1.4 μm. CPD and electric field signals measured using many-pass technique allowed us to estimate the influence of electrostatic field disturbance, especially, in the case of small objects.

Keywords: work function, contact potential measurement, electric field measurement, Kelvin probe, Scanning probe microscopy, imaging of surface electrical properties, surface interfacial characterization, microelectronic characterization

PACS numbers:

68.37.Ps Atomic force microscopy (AFM)

68.35.Ct Interface structure and roughness

73.40.Cg Contact resistance, contact potential

1. Introduction

The contact potential difference (CPD) between two materials is closely related to their work functions, but usually CPD is influenced by adsorption or oxide layers if measured at ambient conditions [1]. A common method to measure CPD in air is based on the vibrating capacitor method or Kelvin method [2]. Commercially available macroscopic Kelvin probe instruments (MKP) have smallest probe diameter about 50 μm, which limit their lateral resolution to about 100 μm. However, CPD resolution of such instruments is very high being about a few mV [3]. Photo-electron emission spectroscopy may be used to obtain spatially resolved maps of work function with high accuracy, but it requires vacuum conditions [4]. Scanning Kelvin probe microscopy (SKPM) is successfully employed for CPD measurements of micron or submicron objects [5, 6], but there is a number of delicate moments concerning measurement itself and data interpretation as well. SKPM lateral resolution depends on probe geometry, tip quality, tip-surface distance, and feedback fine tuning [7-9].

Opposite to MKP instrument, SKPM is sensitive to local change of electric field, caused for example by sharp topographic features, steps and other topography changes [2, 10]. In most works, authors compare SKPM results with either literature data or with data measured by photo-electron emission spectroscopy [8, 11-13]. Taking into account large variations of measured values of work function for the same material prepared by different methods and characterized by different techniques, it is desirable to measure the same sample in similar conditions (in our case, at ambient conditions). Besides it is known, that CPD signal, measured by SKPM, is size dependent and generally shows smaller values on submicron objects [2, 14]. Also a reduction of the work-function value has been observed in the vicinity of steps and edges on highly oriented pyrolytic graphite and metals [15].

In this work we compare CPD values measured by MKP and SKPM techniques at ambient conditions.

2. Experimental

Several types of samples were used in the experiments. Samples of the first type, used to compare MKP and SKPM techniques, were prepared by thermal evaporation of Al, Ni or Pt metal films on indium tin oxide (ITO) covered glass (*Sidrabe*). In these samples one region was a macroscopic metal stripe for MKP

measurements, whereas the second region was an array of metal islands, deposited through a contact mask. We used 600 and 2000 mesh TEM Cu grid (*Agar*) as a shadow mask. The second type of samples, used to investigate Kelvin signal degradation upon a decrease of object size, was Au/Cr patterns on a Si wafer, formed by electron beam lithography (EBL). Tescan Vega II LMU scanning electron microscope equipped with nanolithography system Raith Elphi Plus was used for EBL writing. Patterns were written with a dose 990 mC/cm^2 on Si wafer (*Raith*) spin-coated with 300 nm thick PMMA 495K resist. After developing, samples were coating with 20 nm Cr (adhesion layer) and 40 nm Au (top layer) using thermal evaporation (10^{-5} torr). Lift off procedure was performed in hot acetone during 30 min.

Macroscopic Kelvin probe (MKP) measurements were performed by SKP5050 instrument (*KP Technology*) using 2 mm Au probe. Scanning probe microscope (SPM) "SMENA-A" (*NT-MDT*) was used for microscopic measurements in standard AFM/SKPM/EFM modes using many-pass technique. Different Pt coated tips (NSC35 type, *Mikromasch*), having a resonance frequency in the range from 90 to 250 kHz, were used. The samples topography was acquired using the tapping mode AFM during the first scan line (no voltage has been applied during scanning). Next, Kelvin probe images were obtained in SKPM mode during the second scan line at typical lift height of 25 nm, the tip oscillating voltage U_{ac} in the range of 2.5 V, and the dc voltage U_{dc} applied by means of the feedback loop to keep the cantilever oscillation amplitude at the zero level. Finally, electric field images were taken in EFM mode during the third scan line at the lift height of 80 nm, the tip oscillating voltage U_{ac} in the range of 0.75 V, and the bias voltage U_{dc} set to 3.0 V. We set U_{dc}=3.0 V to increase EFM signal and satisfy condition $U_{dc} > U_s$, where U_s is the surface potential. Lift height was chosen as small as possible, but large enough not to touch the surface. Both MKP and SPM measurements were performed at ambient conditions. It is well known, that the work function values measured at ambient conditions may differ from true values measured in UHV. Therefore, the aim of this work was to compare results obtained by two techniques at ambient conditions but not to find the true work function values for the given materials.

3. Results and discussion

Both MKP and SKPM measure CPD using vibrating capacitor principle, where sample and vibrating probe form the two electrodes of a capacitor. MKP measures CPD signal averaged over a region equal to the probe area of about 2 mm in our case. Electric field between MKP probe and a sample is rather homogeneous in contrast to SKPM (Fig. 1).

MKP detects ac-current i_{ac}, induced by the probe vibration [2], and nullify it applying external voltage U_{ext}:

$$i_{ac} = (\Delta\Phi/e - U_{ext})\frac{dC}{dt}, \quad (1)$$

where $\Delta\Phi$ is a work function difference between the tip and the sample, and e is the elementary charge. C is the capacitance of the probe-sample capacitor, which is periodically modulated by a vibrating probe over the sample surface:

$$C = \varepsilon\varepsilon_0 \frac{A}{z_0 + \Delta z \sin(\omega t)}, \quad (2)$$

where A is the Kelvin probe area (macro-probe diameter), ε – the dielectric constant of the medium (the air in the present experiments) between the probe and the sample, ε_0 – the electric constant, ω – the frequency of the probe vibration, z_0 – the probe-sample distance ($z_0 >> \Delta z$), and Δz – the amplitude of the probe vibration. Detailed description of the MKP technique can be found in [2].

Both EFM and SKPM images are constructed from the first harmonic (1ω) component of force F acting between tip and sample surface [16]:

$$F_{1\omega} = C_t E_s U_{ac} + \partial C_t/\partial z\,(U_{dc} - U_s)\,U_{ac} \quad (3),$$

where C_t is the capacitance of the tip-surface configuration, $E_s = \sigma/\varepsilon_0(1 + \kappa)$ is the field due to an infinite sheet of uniform charge σ, κ is the dielectric constant of sample material, $\partial C_t/\partial z$ is the partial derivative of the tip-surface capacitance with respect to the tip-surface separation, U_{dc} and $U_{ac}=U_1\sin(\omega t)$ are the dc and ac voltages applied to the tip, and U_s is the surface potential or contact potential. EFM is also called open-loop SKPM. In contrast, SKPM mode use feedback loop, where U_{dc} is varied to nullify the force, so that F=0 at $U_{dc}= U_s=\Delta\Phi/e$.

In standard SKPM mode, CPD is measured during the second scan (the so-called, Lift mode), when the tip is lifted of 10-100 nm above the sample surface, and the tip trajectory follows the AFM topography profile, which was recorded during the first scan. The smaller is the tip-surface separation; the better is CPD resolution [8].

However, the influence of topography becomes more pronounced at close distances. The problem is related to the electric field tending to concentrate at the sharp protrusions or steps. Therefore, even Lift mode is not able to compensate fully an increase of electric field at the edge of protruding objects. First term in equation 3 describes electrostatic interaction of a tip with flat surface, where E_s is uniform electric field produced by an infinite sheet of uniform charge σ. Let us suppose that one has a sample surface with some sharp features on top and applies some voltage to the sample. As a result, electrons will be redistributed over surface, and electric field will be concentrated at sharp features. The electrostatic force acting on AFM tip will be higher over sharp features in comparison to the force over flat surface. It means that AFM tip will sense different voltage values in the two regions. Therefore, when SKPM signal is normalized to the value at the flat region, artefacts will appear on SKPM images above sharp features (for example, some are marked by arrows in Figs. 2b,c). The CPD value correlates with topographic height of the Pt particles, observed as bright points in Fig. 2b: it is larger for the higher particles. For example, the height of the particle No.1(No.2) is 18(98) nm, and its CPD is by 33(160) mV larger than that of the flat Pt region. Note that in order to minimize the electrostatic contribution to the topographic signal, U_{ac} used to oscillate tip during SKPM has to be as small as possible.

To exclude the influence of topography on SKPM signal, we prepared metallic (Al, Ni or Pt) islands with lateral size l=25 μm much larger than their height h=50 nm ($l >> h$). A region of small islands was formed for SKPM measurements using shadow mask technique at one side of the sample (Fig. 2a), whereas a large metal stripe was prepared at the other side of the same sample for MKP measurements. The shadow mask technique was used because sample surface is not treated by any chemicals and thus cannot be contaminated.

Three different metals Al, Ni and Pt, having the work function values of 4.2-4.26 eV for Al, 5.04-5.35 eV for Ni and 5.12-5.93 eV for Pt [17-20], were deposited on ITO substrate, having the work function value of 4.7-5.2 eV [21, 22]. Contamination of KPFM tip during CPD measuring procedure will change the work function of the tip and, thus, will make obtained results doubtful. While in MKP probe has no physical contact with a sample during measurement, the KPFM tip is only in gentle contact with sample surface. We choose Pt coating of the tip to make it chemically inert. So, a change of tip material is possible only in case if tip will pick

up some material at the sample surface. Samples for comparison of microscopic and macroscopic Kelvin Probe were prepared without any organic chemicals and we choose ITO as substrate coated with Pt, Ni and Al. Indium tin oxide is hard and chemically inert material [23]. It is known that Al is coated by thin compact Al_2O_3 film at ambient conditions [24]. Pt is exactly the tip coating material and cannot contaminate the tip. Ni is the less reliable material from our list [25], however we believe that the tip contamination will be negligible during tip scanning over the surface in Tapping mode. Therefore, we suppose a high degree of confidence of our CPD measurement results.

Typical MKP measurement was 2-3 scan lines over metal/ITO stripe, and the average CPD value was calculated. In SKPM mode, a set of images, showing a variation of CPD signal and AFM topography, were recorded at different magnifications. Results are summarized in Table 1. CPD values measured by SKPM were about 10-30% smaller compared to the values obtained by MKP method. Probably, CPD signal measured by SKPM was lower due to the long range electrostatic interaction of the tip cone and the cantilever itself with the sample surface [8]. However, the agreement between two methods is satisfactory and reproducible.

Table 1. Comparison of CPD values measured by MKP and SKPM for different samples.

CPD (V)	Al / ITO	Ni / ITO	Pt / ITO
MKP	1.17±0.008	0.37±0.008	-0.047±0.004
SKPM	0.88±0.03	0.27±0.026	-0.042±0.005

The use of shadow mask deposition technique did not allow us to create metal islands with sharp edges. Therefore, Au/Cr patterns were prepared on Si wafer using electron beam lithography to estimate a decrease of the CPD signal measured in SKPM mode upon a decrease of object size (Fig. 3). Large amount of fabricated figures gives us an opportunity to obtain sufficient number of images and to exclude damaged objects. Cr underlayer provides good adhesion especially for small objects and prevents their displacement by AFM tip during scanning. Physisorbed Au particles displacement caused by the tip movement occurs frequently both on HOPG and Si wafer surfaces.

We focused our attention on two types of objects, as most appropriated for an investigation of the CPD dependence on the object area. They are the isosceles triangles with acute angle and a set of circles of different diameters. Taking into account spherical symmetry of tip-surface interaction, the circle shaped objects are well suited to find quantitative CPD dependence on the object size. In Fig. 4 one can see circles and ellipses of different size. Au (5.3-5.47 eV) has higher work function than Si (4.6-4.85 eV) [17-18] and, thus, objects appear dark (Figs. 4 and 5). CPD signal from the largest circle, having a diameter of 1.4 μm, has rather flat profile at the centre, whereas the CPD signal decreases for smaller circles and ellipses. Moreover, upon a decrease of object lateral size the edge related artefacts [10, 15] become more pronounced (Fig. 4b). To estimate the influence of electric field disturbance on edges and protrusions, the CPD and EFM signals were measured simultaneously with topography AFM signal (Figs. 4b,c).

In both cases, the microscope measures the force caused by electric field at the cantilever resonance frequency. In EFM one can obtain the same signal, which is used for feedback loop operation during CPD measurement. We applied U_{dc}=3 V during EFM measurement, which is higher, than CPD difference between Au and Si (0.1-0.15V) $U_{dc}>U_s$, in order to decrease EFM material related sensitivity. Actually, CPD signal measured by SKPM is a superposition of the true CPD and EFM signals (as well as EFM signal itself contains CPD signal). For demonstration of the electric field disturbance effect, we plotted CPD and EFM signals on one graph (Fig. 4d). In the ideal case for CPD measurement, there should be no contrast in the EFM image to have a correct CPD signal. Thus, the EFM image may be used to estimate disturbance degree of the CPD signal.

However, we cannot precisely follow the decrease of CPD signal upon the decrease of objects size due to strong edge effects. To overcome this problem, one can use triangles with acute angle instead of set of circles with different size (Fig. 5). Here the region on Si wafer close to the triangle appears darker than far from that. This effect caused by long-range electrostatic interaction, which is the main reason of CPD signal dependence on the object size. We found what CPD signal starts to drop when triangle base size becomes smaller than about 1.4 μm. Note, that this result was obtained for a given type of AFM tips; and for tips of another type results may be different. CPD signal decrease may be represented as a function of triangle base size (Fig. 5d).

We believe that CPD results performed by conventional SKPM instrument and conventional tips at ambient conditions on objects smaller than about 1 μm may be used only for qualitative or comparative measurement; otherwise both edge artefacts and CPD dependence on object size need to be taken in account.

4. Summary

Contact potential difference on the same samples was measured by macroscopic Kelvin probe instrument and scanning Kelvin probe microscope at ambient conditions. CPD values measured by SKPM were about 10-30% smaller then the values obtained by MKP method. CPD signal dependence on the object size was investigated on isosceles triangles with acute angle and a set of circle-shaped objects having different diameters. We found that the CPD signal starts to decrease when object size becomes smaller than about 1.4 μm. The EFM signal measured simultaneously with the CPD ones helps to estimate the influence of electric field especially on sharp topographic features and small objects.

Acknowledgments

The authors are grateful to A.Tokmakov, J.Sipols and V.Kolbjonok for assistance in sample preparation. The work was supported by ESF Project 2009/0202/1DP/1.1.1.2.0/09/APIA/VIAA/141.

References

1. C. Sebenne, D. Bolmont, G. Guichar, M. Balkanski, Phys. Rev. B. **12,** 3280 (1975)
2. M. Rohwerder, F. Turcu, Electrochim. Acta. **53,** 290 (2007)
3. I. Baikie, S. Mackenzie, P. Estrup, J. Meyer, Rev. Sci. Instrum. **62,** 1326 (1991)
4. W. Telieps, E. Bauer, Ultramicroscopy. **17,** 57 (1985)
5. H. Jacobs, A. Stemmer, Surf. Interface Anal. **27,** 361 (1999)
6. T. Glatzel, H. Steigert, S. Sadewasser, R. Klenk, M. Lux-Steiner, Thin Solid Films. **480–481,** 177 (2005)
7. M. Zhao, V. Sharma, H. Wei, R. Birge, J. Stuart, F. Papadimitrakopoulos, B. Huey, Nanotechnology. **19,** 235704 (2008)
8. H. Jacobs, P. Leuchtmann, O. Homan, A. Stemmer, J. Appl. Phys. **84,** 1168 (1998)
9. H. Jacobs, H. Knapp, A. Stemmer, Rev. Sci. Instr. **70,** 1756 (1999)

10 E. Tevaarwerk, D. Keppel, P. Rugheimer, M. Lagally, M. Eriksson, Rev. Sci. Instr. **76,** 053707 (2005)

11. U. Zerweck, C. Loppacher, T. Otto, S. Grafström, L. Eng, Phys. Rev. B. **71,** 125424 (2005)

12. M. Bohmisch, F. Burmeister, A. Rettenberger, J. Zimmermann, J. Boneberg, P. Leiderer, J. Phys.Chem. B. **101,** 10162 (1997)

13. M. Nonnenmacher, M. O'Boyle, H. Wickramasinghe, Appl. Phys. Lett. **58,** 2921 (1991)

14. T. Glatzel, S. Sadewasser, M. Lux-Steiner, Appl. Surf. Sci. **210,** 84 (2003)

15. C. Sommerhalter, T. Matthes, T. Glatzel, A. Jäger-Waldau, M. Lux-Steiner, Appl. Phys. Lett. **75,** 286 (1999)

16. S. Kalinin, A. Gruverman, *Scanning Probe Microscopy: Electrical and Electromechanical Phenomena at the Nanoscale* (Springer, 2006) p. 694.

17. D. Lide, *CRC Handbook of Chemistry and Physics* (CRC Press, Boca Raton, 2004)

18. J. Riviere, M. Green, *Work Function: Measurements and Results, Solid State Surface Science* (Decker, New York, 1969)

19. H. Michaelson, J. Appl. Phys. **48,** 4729 (1977)

20. J. Hölzl, F. Schulte, *Work Functions of Metals, in Solid Surface Physics* (Springer-Verlag, Berlin, 1979)

21. S. Kim, J. Jang, B. Chin, J. Lee, Curr. Appl. Phys. **8,** 475 (2008)

22. C. Kim, B. Lee, H. Yang, H. Lee, J. Lee, H. Shin, J. Kor. Phys. Soc. **47,** S417 (2005)

23. K. Zenga, F. Zhua, J. Hua, L. Shena, K. Zhanga, H. Gongb, Thin Solid Films. **443,** 60 (2003)

24. A. Hasnaoui, O. Politano, J. Salazar, G. Aral, Phys. Rev. B. **73,** 035427 (2006)

25. G. Allen, P. Tucker, R. Wild, Oxid. Met. **13,** 223 (1979)

Figure captions

Figure 1. Schematics of electric field distribution in MKP and SKPM measurements.

Figure 2. (Color online) Metal Pt islands on ITO: (a) optical image; (b) AFM topography, z range 70 nm and (c) CPD signal, z range 170 mV.

Figure 3. (Color online) SPM images of Au objects on Si substrate: (a) AFM topography and (b) CPD signal.

Figure 4. (Color online) SPM images of Au circles and ellipses on Si substrate: (a) AFM topography, z range 150 nm; (b) CPD signal; (c) EFM signal; (d) CPD and EFM cross section profiles.

Figure 5. (Color online) SPM images of Au triangles on Si substrate: (a) AFM topography, z range 150 nm; (b) CPD signal; (c) cross section; (d) CPD signal decrease as function of triangle base size: diamonds is experimental data and solid line is second order polynomial fit.

Figures

Figure 1.

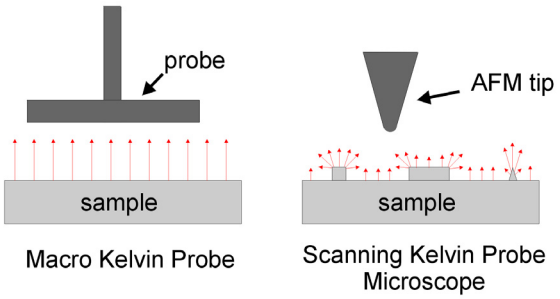

Figure 2.

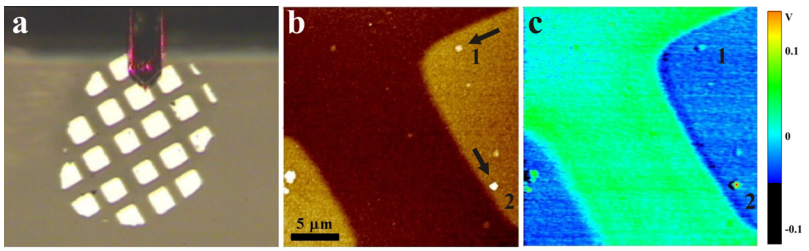

Figure 3.

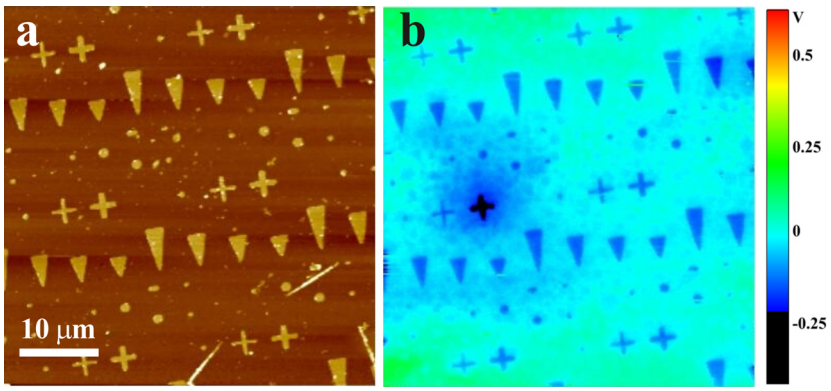

Figure 4.

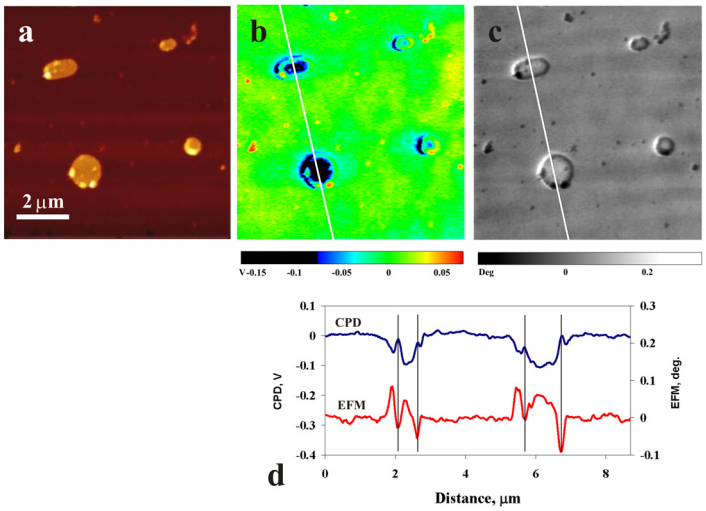

Figure 5.